Journal of Lasers in Medical Sciences

J Lasers Med Sci 2023;14:e69

Original Article

http://journals.sbmu.ac.ir/jlms

doi 10.34172/jlms.2023.69

Blue Laser-Activated Silver Nanoparticles from Grape Seed Extract for Photodynamic Antimicrobial Therapy Against *Escherichia coli* and *Staphylococcus aureus*

Ahmad Khalil Yaqubi, Suryani Dyah Astuti*, Andi Hamim Zaidan, Dezy Zahrotul Istiqomah Nurdin

Department of Physics, Faculty of Science and Technology, Airlangga University, Surabaya, 60115, East Java, Indonesia

***Correspondence to**
Suryani Dyah Astuti,
Email: suryanidyah@fst.unair.ac.id

Received: September 22, 2023
Accepted: November 15, 2023
ePublished: December 29, 2023

Abstract

Introduction: Living organisms, particularly humans, frequently encounter microorganisms like bacteria, fungi, and viruses in their surroundings. Silver nanoparticles are widely used in biomedical devices due to their antibacterial, antifungal, and antiviral properties. The study evaluates the efficacy of blue laser and silver nanoparticles from grape seed extract (AgNPs-GSE) in reducing gram-negative *Escherichia coli* and gram-positive *Staphylococcus aureus* bacteria causing infections.

Methods: The sample consisted of four groups: a control without laser irradiation (T0), *E. coli* samples (A1 and A2) irradiated with a 405 nm diode laser at different times and concentrations of silver nanoparticles, and *S. aureus* samples (A3 and A4) irradiated with a 405 nm diode laser at different times and concentrations. Bacteria in groups A2 and A4 were treated with a photosensitizer (PS) made from grape seed extracts, incubated for 10 minutes, and then irradiated for 90, 120, 150, and 180 seconds. The samples were cultured on Tryptic Soy Agar (TSA) media, incubated at 37 °C, counted by using a Quebec colony counter, and analyzed using ANOVA and Tukey tests with a significance level of $P<0.05$.

Results: The study found that 10 µl of AgNPs-GSE, when combined with exposure to a blue laser at 405 nm and a dose of 3.44 J/cm², can effectively photoinactivate *E. coli* and *S. aureus* bacteria. The addition of AgNPs-GSE to *E. coli* bacteria led to a significant reduction in their viability, with a reduction of 73.93%, 80.96%, and 83.80%, respectively. Similarly, when *S. aureus* bacteria were irradiated for 180 seconds by adding 1 mM, 1.5 mM, and 2 mM AgNPs-GSE, bacterial viability was reduced by 70.87%, 78.04%, and 87.01%, respectively.

Conclusion: The findings from the present study indicate that at an energy density of 3.44 J/cm², it was possible to inactivate *E. coli* by 83.80% and *S. aureus* by 87.01%.

Keywords: Silver nanoparticles; Grape seed extract; Antibacterial; Laser therapy; Laser wavelength.

Introduction

Nanotechnology encompasses a broad domain that spans biology, chemistry, physics, and engineering. The term "nano" originates from the Greek word meaning "dwarf," and it refers to particles with dimensions ranging from 1 to 100 nm.[1] A nano unit, equivalent to one billionth of a meter, is a key component of nanotechnology, which involves the creation of nanoparticles with diverse sizes, shapes, and structures. These nanoparticles have unique physical properties due to their minimal dimensions and large surface area.

These unique characteristics encompass attributes such as electricity, magnetism, and optics.[2] The bio-manufacturing of nanoparticles is a particularly dynamic field within nanoscience and technology.[3] Various chemical and physical methods produce nanoparticles, including metals like silver. However, these processes are costly and have adverse environmental impacts.[4,5]

Silver nanoparticles (AgNPs) have garnered considerable interest due to their unique characteristics, which include significant reduction capabilities, photoelectrochemical reactivity, favorable electrical conductivity, and antibacterial properties. In addition to applications in agriculture, biosensors, and textiles, AgNPs have been expanded to include water disinfection.[6] Ultrasonic radiation,[7] laser ablation,[8] evaporative cooling,[9] chemical vapor deposition,[10] explosion-induced synthesis,[11] impregnation,[12] co-precipitation,[13] sol-gel,[14] deposition-precipitation,[15] microwave,[16] and microorganisms[17] are only a few of the processes used to create AgNPs. However, it has become necessary to synthesize them in more cost-effective and environmentally benign ways.

One highly favored ecologically conscious method involves creating AgNPs by applying plant extracts as both reductive and stabilizing agents. Numerous plant varieties, such as *Jatropha curcas, Capsicum*

Please cite this article as follows: Yaqubi AK, Astuti SD, Zaidan AH, Nurdin DZI. Blue laser-activated silver nanoparticles from grape seed extract for photodynamic antimicrobial therapy against *Escherichia coli* and *Staphylococcus aureus*. *J Lasers Med Sci.* 2023;14:e69. doi:10.34172/jlms.2023.69.

annuum, Argemone mexicana, Ocimum sanctum, Ficus benghalensis, and *Hibiscus rosa-sinensis*, have proven effective in transforming silver ions (Ag^+) into metallic silver (Ag^0) nanoparticles.[18] Recent studies highlight the potential of AgNPs, cost-effective agricultural waste materials, for anti-cancer, antioxidant, and biofilm properties, used in water treatment, textiles, food preservation, and medical applications.[19]

AgNPs, when attached to a photocatalyst surface, exhibit antimicrobial properties through DNA modifications, enzyme deactivation, and cellular disruption.[20] AgNPs were observed to engage in a reaction similar to Fenton chemistry, facilitating the degradation of 17-Ethinyl estradiol and bisphenol A in water.[21] As an illustration, grape skin, stalk, and seed residues from grape processing were used to produce silver and gold nanoparticles.[22] These silver nanoparticles exhibited superior antibacterial efficacy compared to eight strains of both Gram-negative and Gram-positive bacteria.

Grape seed extract, rich in secondary metabolites and polyphenolic compounds, exhibits antibacterial properties against both gram-negative and gram-positive bacteria.[23] Grape seeds, rich in vitamins C and E, flavonoids, and other beneficial elements, are used in skincare products and professional treatments. In contrast, grape seed extract and flesh contain proanthocyanins and resveratrol.[24] The size of AgNPs significantly influences their properties, but the influence of reaction conditions like temperature on environmentally friendly synthesis using grape seed extract needs to be thoroughly explored.[25]

Furthermore, their catalytic capability in disintegrating hazardous organic dyes under aqueous conditions has only been sporadically documented.[26] The study investigates the creation of AgNPs using grape seed extract at various reaction temperatures and its antibacterial efficacy against *E. coli* and *S. aureus* bacteria, using UV-Vis assay and disc diffusion methods over a 24-hour incubation period.

Additionally, a supplementary facet of this research entails applying antimicrobial photodynamic therapy (aPDT) using a blue laser. This aspect aims to observe the impact of exposing the sample to the blue laser for a specific duration. The rationale behind selecting the blue laser for photoinactivation stems from the absorption spectrum of silver nanoparticles, which spans between 400 nm and 500 nm, and Grape Seed Extract's absorption spectrum, which covers a range of approximately 200 nm to 800 nm. This correspondence renders blue lasers particularly suitable for this experimental context.

Materials and Methods

Characterization of UV-Vis Spectrophotometer

The UV-Vis spectrophotometer was used to evaluate the absorption behavior of silver nanoparticles (AgNPs-GSE) in the visible light range of 325 nm to 600 nm, specifically in the presence of *E. coli* and *S. aureus*, revealing a specific wavelength absorption capacity and characterization process.

The Laboratory of Biophysics and Medical Physics at Airlangga University conducted UV-Vis spectrophotometer characterization for measuring absorbance using a Shimadzu 1800 Spectrophotometer. The process captured wavelengths from 300 to 1000 nm, resulting in absorbance values.

Nanoparticle Stability

A stability test on silver nanoparticles evaluated their size and distribution after synthesis. The test involves placing the nanoparticles in a glass container, sealing it, and storing it at room temperature. Physical color changes and UV-Vis spectrophotometry analysis were used to assess stability after 24 hours and one week.

Spectrophotometry is a valuable method for tracking nanoparticle stability, but it has limitations. UV-Vis spectrophotometry can determine the average size and distribution of silver nanoparticles, and it can indirectly evaluate color changes in nanoparticles.

Antibacterial Activity Test

The test examines the antibacterial properties of AgNPs-GSE using disc diffusion as a standard method. This method, typically performed aerobically, is suitable for assessing antibacterial activity, as common bacteria like *E. coli* and *S. aureus* thrive in oxygen-rich conditions, making it suitable for testing antibacterial effectiveness.

The first step involved culturing bacteria in sterile Tryptone Soy Broth (TSB) and incubating them for 24 hours. After culture, 50 µL was spread evenly in a 9 cm petri dish, adding Tryptic Soy Agar (TSA) media and waiting for the media to solidify.

Ten microliters of grape seed extract was applied to four 0.5 cm diameter paper discs, and then they were transferred to an agar medium in a petri dish. We placed them equidistantly within one cup, aligned them with the four quadrants, and incubated them for 24 hours.

An inhibition zone around the paper discs indicates the antibacterial activity of grape seed extract.

Bacterial Growth with AgNPs-GSE

To initiate bacterial growth, we prepared 8 ml of sterile TSB media in a test tube, isolated *E. coli* and *S. aureus* bacteria from agar, inoculated them onto 4 mL of TSB media, and incubated them for 24 hours.

After incubation, we took 100 µL of the bacterial culture and added 25 µL of AgNPs-GSE. We transferred this mixture to a microplate and placed it in an incubator at 37 °C for 30 minutes.[27]

Following incubation, we took 50 µL of the mixture and placed it in a petri dish. We incubated the petri dish at 37 °C for 24 hours. Finally, we assessed the reduction in bacterial colonies by conducting a total plate count (TPC).

Irradiation of Bacteria With a Laser

After growing the bacteria with a photosensitizer (silver nanoparticles) for 2 hours, the bacteria were now ready to be exposed to laser light. The irradiation was carried out at an optimal fixed distance from the sample and the light source, perpendicular to each other.

The laser diode was characterized by using a blue laser with a wavelength of 405 nm. The peak wavelength was determined by using a Jasco CT-10 monochromator. The power output was measured at 2.49 mW by an OMM-6810B-220V power meter. The spot beam area was 0.13 cm^2. Diode laser irradiation was performed for varying durations.[28]

$$\text{Energy Density (J.cm}^{-2}\text{)} = \text{Intensity (W.cm}^{-2}\text{)} \times \text{Irradiation Time (s)}$$

The first step of irradiation involved preparing a culture containing 0.5 mL of bacteria and photosensitizer and diluting it in 4.5 ml of sterile physiological water according to the standard dilution that was done previously.[29] We took 50 µL of the dilution and placed it into a sterile cup with a diameter of 3.5 cm. We repeated this process five times for both the second treatment group and the positive control group.

To conduct scientific research, we irradiated each petri dish with a photosensitizer at a 1 cm distance and 90-degree angle, ensuring uniform and controlled exposure. This setup was crucial for consistent and reproducible conditions. Next, we added sterile TSA media to each petri dish and distributed it evenly. After solidifying, we incubated the petri dishes at 37 °C for 24 hours.

For the first treatment and control groups, we used bacterial culture in 9 mL of TSB incubated previously. The first treatment group underwent the same irradiation method as the second and third groups.

Statistical Analysis

After exposure to the blue laser, the number of bacterial colonies was counted by using the TPC plating method. The obtained results were recorded as quantitative data. To calculate the percentage decrease in the number of bacterial colonies, we used the following equation:

$$\%Colony\ decline = \left| \frac{\sum treatment - \sum control}{\sum control} \right| x100\ \%$$

The study utilized IBM SPSS for quantitative data analysis, employing a two-way ANOVA factorial test to determine the effect of factors and their interaction. The test required normally distributed data and minimal interval scale data, with a significant difference defined as $P < \alpha = 0.05$. Tukey's post hoc test and Kolmogorov-Smirnov test were used to check data normality.

Results

Silver Nanoparticle Characterization Results

Characterization of UV-Vis Spectrophotometer

The test results revealed the absorbance value of AgNPs-GSE at visible light wavelengths, with UV-Vis absorption spectrum measurements conducted between 325 nm and 600 nm. Figure 1 shows the results plotted against the visible light wavelength.

Stability of Nanoparticles

The physical stability of AgNPs-GSE can be visually observed through the color of the solution. Figure 2a displays the golden yellow color of AgNPs-GSE on day 1. Figure 2b shows the visual appearance of AgNPs-GSE on day 7, which has slightly changed from a darker shade to a brownish yellow. No visible agglomeration of the samples occurred after being left for one week. This suggests the absence of large particle sizes.

The wavelength absorbance of AgNPs-GSE was analyzed using UV-Vis on day one and week one after synthesis. Figure 3 illustrates that the absorbance of AgNPs-GSE exhibits good stability. This is evident because the wavelength of the absorbance peak in the UV-Vis

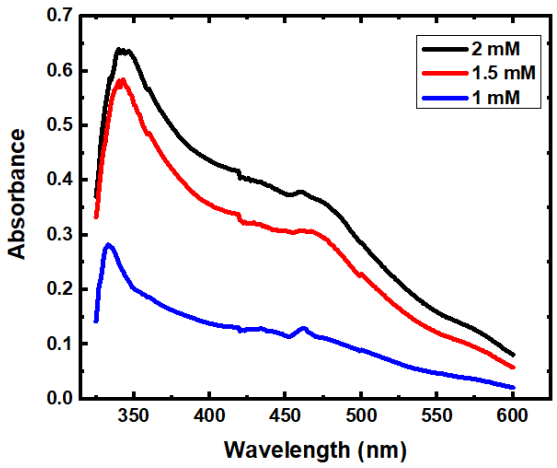

Figure 1. UV-Vis Absorbance Spectrum of AgNPs-GSE at Concentrations of 1 mM, 1.5 mM and 2 mM

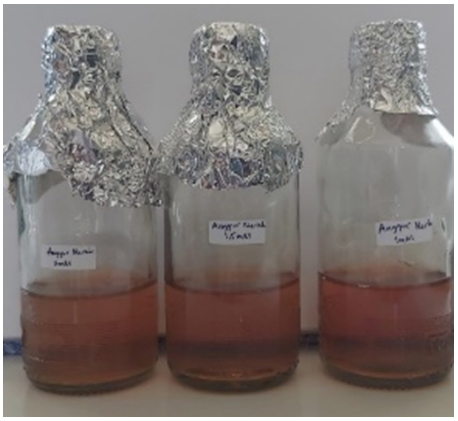

Figure 2. Physical Properties of AgNPs-GSE on (a) Day 1 and (b) Day 7

test does not shift. The peak absorbance spectrum after a week was nearly identical to the absorbance spectrum obtained during synthesis on day 1, which was around 350 nm for 1 mM, 1.5 mM, and 2 mM AgNPs-GSE.

Antibacterial Activity Test Results

An antibacterial test against *Escherichia coli* and *Staphylococcus aureus* was conducted to determine the diameter of the inhibition zones on the growth of bacterial colonies. Each sample was tested using the diffusion well method. The results revealed the presence of inhibition zones with 1 mM, 1.5 mM, and 2 mM AgNPs-GSE antibacterials, respectively, for *Escherichia coli*. Similarly, inhibition zones were observed with 1 mM, 1.5 mM, and 2 mM AgNPs-GSE antibacterial for *Staphylococcus aureus*.

The 0.5 cm diameter paper discs were utilized, and the 5.2 mm measurement of the inhibition zone for AgNPs-GSE with *S. aureus* showed that the substance successfully stopped the development of germs within that particular radius surrounding the disc. Figure 4 shows the inhibition zone diameters of AgNPs-GSE against *S. aureus* and AgNPs-GSE against *E. coli*.

Based on the results of the inhibition zone test presented in Table 1 and Figure 4, it is evident that the highest average diameter of the inhibition zone is observed in AgNPs-GSE inhibition of *S. aureus* bacteria, with a value of 5.2 mm. This falls into the strong category compared to its effect on *E. coli*.

Results of Bacterial Growth with AgNPs-GSE

The antibacterial properties of the synthesis method were demonstrated by adding AgNPs-GSE to two bacterial samples, with the number of colonies developed in the presence of AgNPs-GSE on the dish. Figure 5a illustrates the percentage decrease in *E. coli* bacterial colonies, while Figure 5b depicts the percentage reduction in the number of *S. aureus* bacterial colonies.

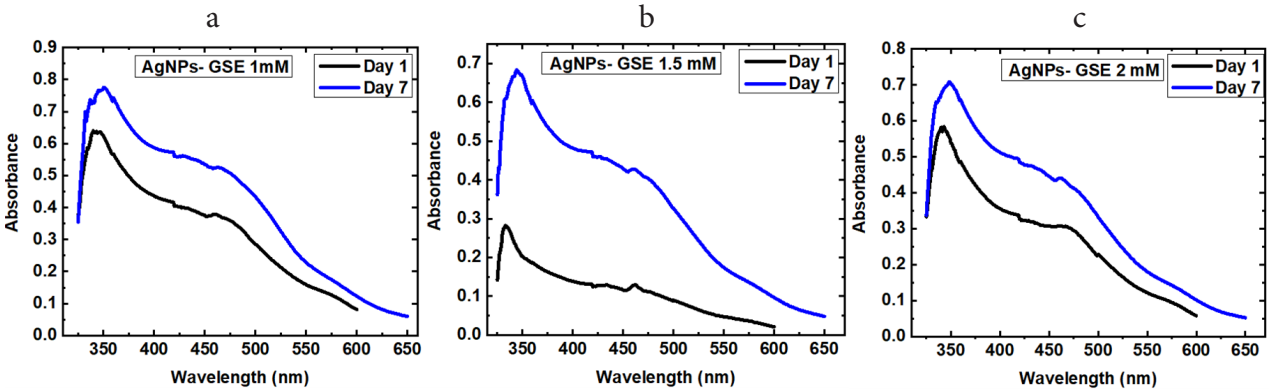

Figure 3. UV-Vis absorbance spectra of AgNPs-GSE day 1 and day 7 (a) 1mM (b) 1.5mM (c) 2mM

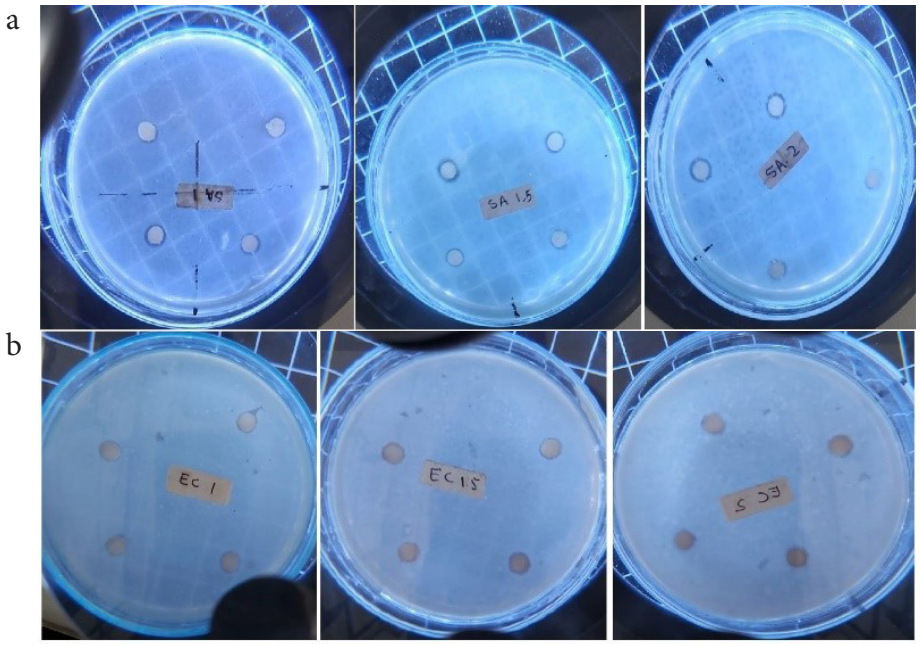

Figure 4. Inhibition Zone Diameters (a) AgNPs-GSE Against *Staphylococcus aureus;* (b) AgNPs-GSE Against *Escherichia coli*

Laser Irradiation Results

The laser irradiation process was conducted with variations in time, precisely 90, 120, 150, and 180 seconds. These different time intervals resulted in varying energy densities for each treatment. The effectiveness of this laser irradiation can be observed through the reduction in the number of bacterial colonies compared to the control group.

Escherichia coli Bactria

There were two treatment groups: the first was irradiated with a laser, and the second was irradiated with a laser in addition to the incorporation of 20% AgNPs-GSE in each concentration variation during the synthesis process in *E. coli* bacteria.

The observational data underwent statistical analysis using a two-way ANOVA factorial test in IBM SPSS, ensuring it met criteria like interval-scale measurements, normal distribution, and homogeneity of variances, validating the data, and allowing comparison with manually calculated results.

The results of the data normality test for the two treatment groups yielded a significance value of $P = 0.837$, more significant than $\alpha = 0.05$. This indicates that the data follow a normal distribution. Subsequently, a data homogeneity test was conducted to determine whether the data exhibited homogeneous variations. The homogeneity test results showed a significance value of $P = 0.677$, also more significant than $\alpha = 0.05$, indicating that the data variations were homogeneous.

Moving on to the two-way factorial ANOVA test, the results showed a significance value of $P = 0.000$, less than $\alpha = 0.05$. This suggests a significant difference in the outcomes between the various time intervals for each treatment. A post hoc test was conducted to identify treatment groups with distinct outcomes, showing significant differences in results at different time intervals.

The two-way ANOVA factorial test showed that laser treatment with 2mM AgNPs-GSE for 180 seconds resulted in the highest percentage of *E. coli* bacteria death at 83.93%. Figure 6 shows a comparison of bacterial death percentages across three treatment groups using laser irradiation at 90, 120, 150, and 180 seconds. The treatment resulted in different energy densities for each treatment. The success was observed in reducing bacterial colonies compared to the control group. AgNPs-GSE was added to each concentration variation during synthesis for *S. aureus* bacteria. The results indicated that the time intervals of 90, 120, 150, and 180 seconds yielded significantly different results, with the percentage of *E. coli* bacterial death being 67.79%, 77.82%, 80.40%, and 83.80%, respectively. A comparison of the percentage of bacterial death across the three treatment groups is illustrated in Figure 6. The conclusions drawn from the statistical test results are presented in Table 2.

Table 1. Inhibitory Zone Measurements of AgNPs-GSE on *Staphylococcus aureus* and *Escherichia coli* Bacteria

No	Sample	Bacteria	Inhibition zone (mm)	Category
1	AgNPs-GSE	*S. aureus*	5.2	Moderate
2	AgNPs-GSE	*E. coli*	3.8	Moderate

Staphylococcus aureus Bacteria

The study involved adding 20% AgNPs-GSE to *S. aureus* bacteria, and a two-way ANOVA factorial test was conducted to assess the impact of each factor, ensuring data met specific criteria for validation and comparison with manual calculations, including an interval scale and homogeneous data variations.

The results of the data normality test for the three treatment groups yielded a significance value of $P = 0.855$, more significant than $\alpha = 0.05$. This indicates that the data follow a normal distribution. Subsequently, a data homogeneity test was conducted to determine whether the data exhibited homogeneous variations. The homogeneity test results showed a significance value of $P = 0.604$, also more significant than $\alpha = 0.05$, indicating

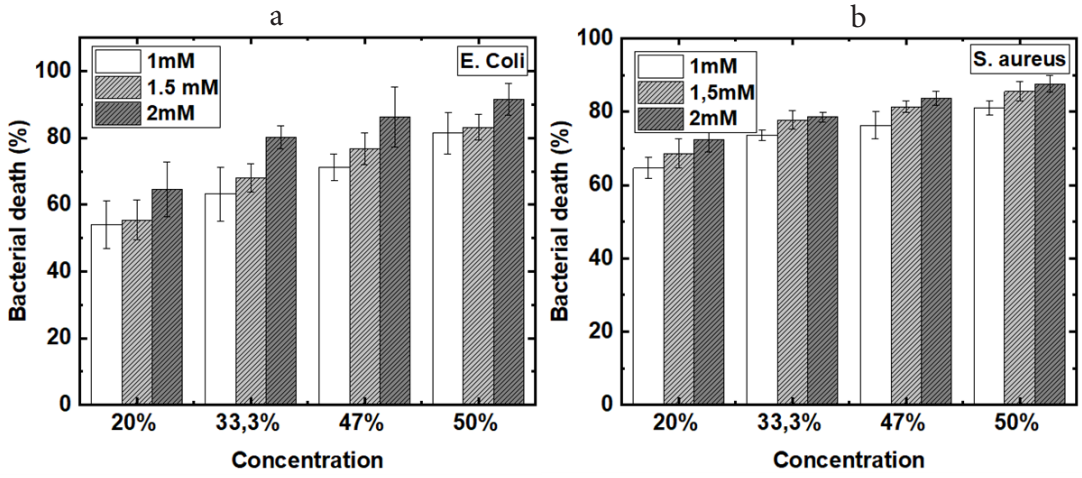

Figure 5. Comparison of the Percentage Reduction of (a) *Escherichia coli* Bacteria and (b) *Staphylococcus aureus* BACTERIA

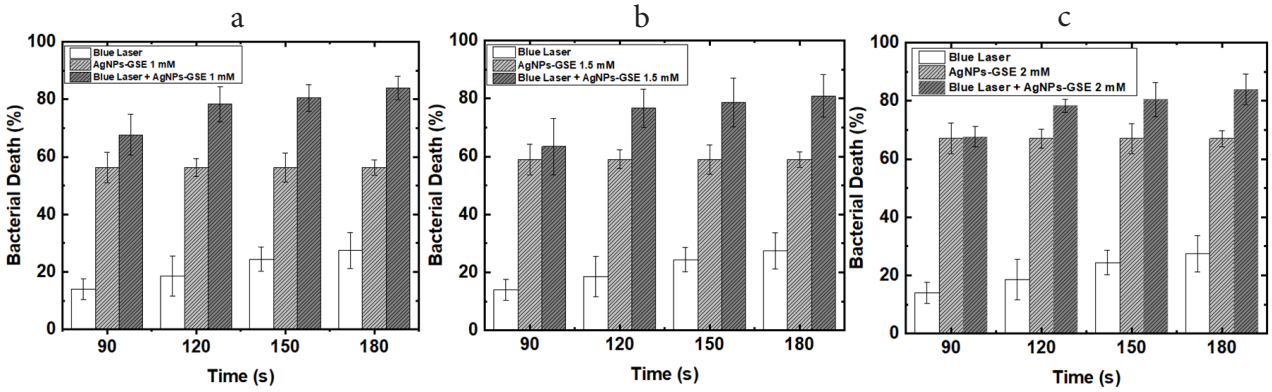

Figure 6. Comparison of the Percentage Reduction of *Escherichia coli* Bacteria With AgNPs-GSE (a) 1mM (b) 1.5 mM (c) 2mM

Table 2. Statistical Analysis Results for *Escherichia coli* Bacteria

Treatment	Group	N	Death Bacteria (%)	
			Average	SD
AgNPs-GSE concentrations	1 mM (1)[1]	20	56.31	3.03
	1.5 mM (2)[1]	20	58.97	7.5
	2 mM (3)[2]	20	67.04	4.48
Total		60		
Time	90 s (A)[1]	15	67.79	8.41
	120 s (B)[2]	15	77.82	8.22
	150 s (C)[3]	15	80.40	6.7
	180 s (D)[3]	15	83.80	4.24
Total		60		
Interaction	1A (3,4,5,6)	5	61.26	
	1B (5,6)	5	63.8	
	1C (6)	5	65.64	
	1D (6)	5	67.79	
	2A (1,2)	5	74.74	
	2B (2,3)	5	76.21	
	2B (2,3)	5	77.82	
	2B (2,3)	5	77.93	
	2B (2,3)	5	78.41	
	2B (2,3)	5	80.4	
	2B (2,3)	5	80.1	
	2B (2,3)	5	83.8	
Total		60		

Note: P = 0.000 (There are different meanings).

that the data variations are homogeneous.

Moving on to the two-way factorial ANOVA test, the results showed a significance value of $P = 0.000$, less than $\alpha = 0.05$. The post hoc test was conducted to identify the distinct outcomes of each treatment group based on the observed differences in outcomes.

The two-way factorial ANOVA test showed that laser treatment with 1mM AgNPs-GSE for 180 seconds resulted in the highest percentage of *S. aureus* bacteria death at 87.01%. A comparison of the percentage of bacterial death across the three treatment groups is illustrated in Figure 7. The laser irradiation process varied in time at 90, 120, 150, and 180 seconds, resulting in varying energy densities for each treatment. The success was observed in reducing bacterial colonies compared to the control group. In the case of *S. aureus* bacteria, AgNPs-GSE was added to each concentration variation during synthesis. The results indicated that the time intervals of 90, 120, 150, and 180 seconds yielded significantly different results, with the percentage of *S. aureus* bacterial death being 63.42%, 67.50%, 72.85%, and 87.01%, respectively. The conclusions drawn from the statistical test results are presented in Table 3.

Discussion

Bacteria, small, single-celled organisms with primitive structures, obtain nutrients and release metabolic byproducts. They have a dense cell membrane, can enter the body through exposed surfaces, and can cause human infections, including gram-negative and gram-positive bacteria.

Traditionally, the synthesis of silver nanoparticles is carried out by using conventional heating methods.[30] Microwave irradiation offers a faster, more efficient, and uniform heating method for silver nanoparticle synthesis compared to time-consuming, uneven heating methods that can cause significant chemical reaction changes.

The microwave heating method is superior to conventional heating for synthesizing AgNPs-GSE due to its consistent production of small, uniform nanoparticles with enhanced antibacterial activity and photodynamic inactivation, which inhibits cellular metabolic processes by interacting with photosensitizer molecules.[31]

The critical elements in applying photodynamic inactivation are fourfold: visible light, light from the Near-infrared (NIR), reactive oxygen species (ROS), and a photosensitizer that acts as a light sensitizer.[32] The photoinactivation process necessitates a match between the spectrum of visible light used and the absorption spectrum of the photosensitizer. Laser is a widely used light source in photodynamic inactivation due to its

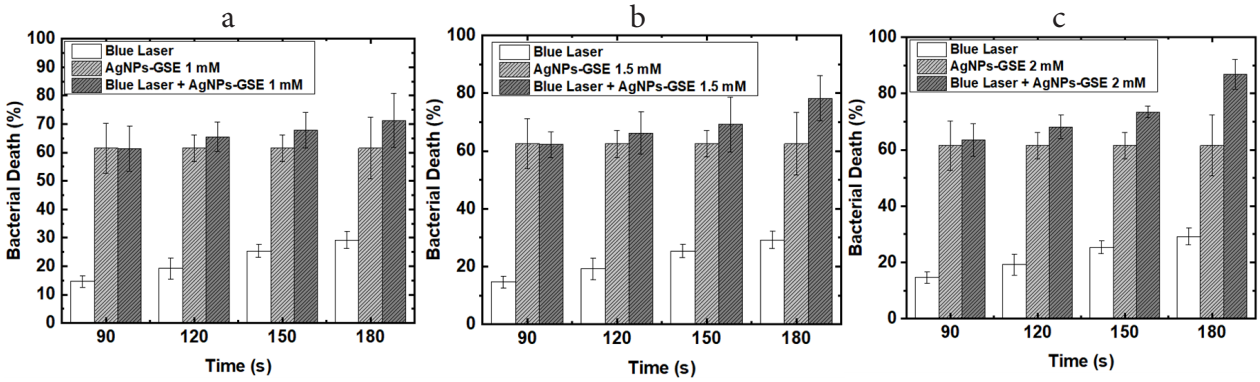

Figure 7. Comparison of the Percentage Reduction of *Staphylococcus aureus* Bacteria With AgNPs-MO (a) 1mM (b) 1.5mM (c) 2mM

Table 3. Statistical Analysis Results for *Staphylococcus aureus* Bacteria

Treatment	Group	N	Death Bacteria (%)	
			Average	SD
AgNPs-GSE concentrations	1 mM [(1)1]	20	61.47	5.33
	1.5 mM [(2)1]	20	62.44	3.33
	2 mM [(3)2]	20	69.01	3.33
Total		60		
Time	90 s (A)[1]	15	63.42	8.41
	120 s (B)[2]	15	67.50	8.22
	150 s (C)[3]	15	72.85	6.7
	180 s (D)[3]	15	87.01	4.24
Total		60		
Interaction	1A [(3,4,5,6)]	5	61.176	
	1B [(5,6)]	5	62.072	
	1C [(6)]	5	63.428	
	1D [(6)]	5	65.362	
	2A [(1,2)]	5	66.428	
	2B [(2,3)]	5	67.508	
	2B [(2,3)]	5	68.096	
	2B [(2,3)]	5	68.832	
	2B [(2,3)]	5	70.872	
	2B [(2,3)]	5	72.85	
	2B [(2,3)]	5	78.042	
	2B [(2,3)]	5	87.012	
Total		60		

Note: P=0.000 (There are different meanings).

numerous advantages, including a uniform and parallel light beam (monochromatic).[33] The study employed lasers for photodynamic inactivation, producing reactive oxygen species at a wavelength matching the absorption spectrum of the photosensitizer. A diode laser with a wavelength of 405 nm was used, with the highest power of 2.49 mW, demonstrating stable output power and preventing excessive heat generation during irradiation at a 1 cm distance.

A *photosensitizer* is a substance that absorbs light with a specific wavelength. Photosensitizers are categorized into two types: exogenous photosensitizers originating from external sources and endogenous photosensitizers originating from within bacteria.[34]

The study utilized two types of photosensitizers: exogenous organic matter-added photosensitizers and endogenous bacteria-produced porphyrin-produced photosensitizers, specifically AgNPs-GSE, with concentrations of 1 mM, 1.5 mM, and 2 mM.

The photoinactivation process involves laser light interacting with AgNPs-GSE, a photosensitizer. Porphyrin molecules absorb photons, causing them to enter the excited singlet state. This temporary state is followed by a triplet excitation state, triggering a crucial photochemical reaction.[35]

The photochemical process involves two pathways: type I and type II. Type I involves an electron transfer between sensitizer molecules and biological molecules, forming radical ions like reactive oxygen species.[36]

In the type II pathway, energy transfers from the excited triplet-state photosensitizer to the triplet-state oxygen, resulting in the formation of excited singlet oxygen.[37] ROS can damage the structure of bacterial cell walls, leading to the lysis of bacterial cells. This represents the initial step in bacterial cell death.[38]

Photochemical processes generate ROS and triplet oxygen radicals, which oxidize unsaturated fatty acids, forming hydroperoxides. These radicals disrupt the formation of saturated fatty acids, resulting in toxic hydroperoxides known as lipid peroxidation. This damage to the bacterial cell wall leads to cell lysis.[39] Table 4 presents findings from photodynamic research on bacterial inactivation using a blue laser.

Astuti et al utilized a blue LED with a wavelength of 430nm and an irradiance of 135 J/cm². Porphyrins were employed as the photosensitizer, resulting in a bacterial death rate of 71.96% for *S. aureus*.[40] Subsequent work by Astuti et al utilized LED light at 417nm with a fluence of 16.19 J/cm², employing curcumin as the photosensitizer and achieving a significantly higher bacterial inactivation rate of 91.49%.[41] Astuti et al employed a diode laser emitting light at 450 nm with an irradiance of 6.13 J/cm².

This time, AgNPs were utilized as the photosensitizer, leading to a bacterial death rate of 64.48% for *C. albicans*.[42] Yaqubi et al used a purple LED with a wavelength of 395 nm, achieving a remarkable 94.3% bacterial inactivation rate for *E. coli* through porphyrins.[43] Figure 8 elucidates the intricate mechanism underlying bacterial inactivation through photodynamic processes.

The study analyzed the effects of varying irradiation durations on *E. coli* and *S. aureus* bacteria. Results showed a decrease in bacterial colonies and an increase in bacterial deaths, with longer irradiation times leading to the higher production of reactive oxygen species and more bacterial deaths.[44]

Research on bacterial photoinactivation using a 405 nm wavelength laser showed that it was more effective for *S. aureus* bacteria. The highest bacterial death rate was achieved at 180 seconds with a dose of 3.44 J/cm^2. *E. coli* had a death rate of 27.45%, while *S. aureus* had a rate of 29.19%. This discrepancy may be due to the distinct cell wall arrangements of gram-positive and gram-negative bacteria.

Gram-positive bacteria like *S. aureus* have a cell wall made of peptidoglycan, teichoic acid, and neuraminic acid, with polysaccharides, making them more susceptible to damage during photoinactivation. In contrast, gram-negative bacteria have a double-membrane system with less peptidoglycan, causing varying responses to photoinactivation.[45]

Gram-negative and gram-positive bacteria produce endogenous photosensitizers that absorb light, triggering photochemical processes that produce ROS. AgNPs-GSE, when combined with laser irradiation, enhances photoinactivation and increases bacterial death, highlighting the effectiveness of external photosensitizers.[46]

Irradiation of *E. coli* bacteria for 180 seconds with the addition of AgNPs-GSE at concentrations of 1 mM, 1.5 mM, and 2 mM, respectively, resulted in a reduction in bacterial death by 73.93%, 80.96%, and 83.80%. Irradiation of *S. aureus* bacteria for 180 seconds with the addition of AgNPs-GSE at concentrations of 1 mM, 1.5 mM, and 2 mM, respectively, resulted in a reduction in bacterial death by 70.87%, 78.04%, and 87.01%. Chlorophyll contains porphyrin, a light absorber with strong structural resistance, which remains intact during irradiation and can absorb light with specific energy levels. AgNPs-GSE is utilized in photodynamic inactivation as a photosensitizer, triggering chemical and biological processes during irradiation. This interaction causes the production of reactive oxygen, which damages bacteria and causes bacterial lysis. The higher the reactive oxygen production, the greater the bacterial death.

Table 4. Photodynamic Research on Bacterial Inactivation With Blue Laser

Research	Source Light	Photosensitizer	Bacteria	Death Bacteria
Astuti et al, (2011)[40]	Blue LED 430 nm 135 J/cm^2	Porphyrins	*Staphylococcus aureus*	71.96%
Astuti et al (2017) [41]	LED 417 nm 16.19 J/cm^2	Curcumin	*Staphylococcus aureus*	91.49%
Astuti et al (2018)[42]	Diode laser 450 nm 6.13 J/cm^2	AgNPs	*C. albicans*	64.48%
Yaqubi et al (2022)[43]	Purple LED 395 nm	Porphyrins	*Escherichia coli*	94.3 %

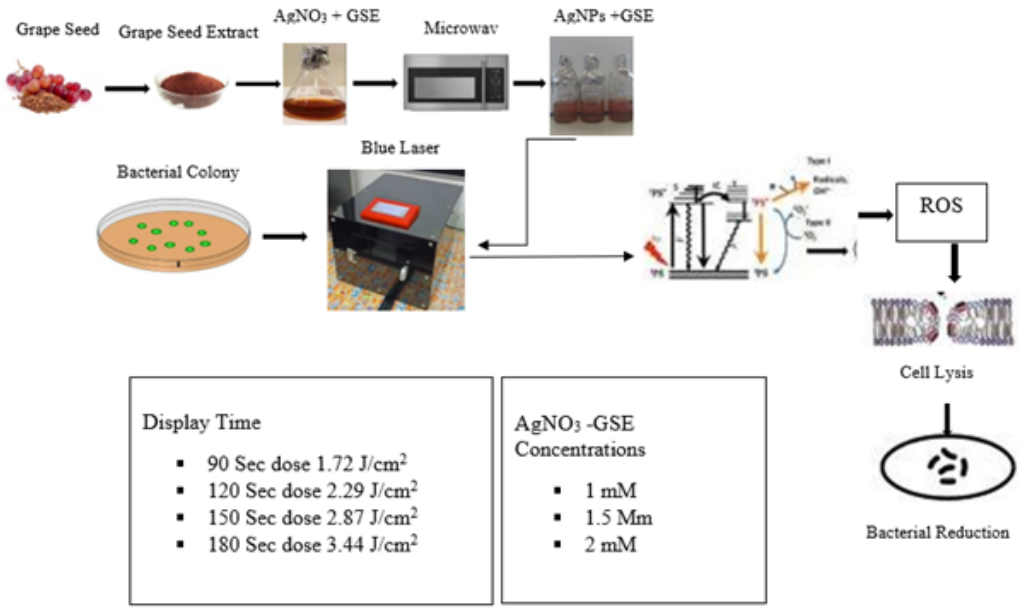

Figure 8. Mechanism of Bacterial Inactivation

Conclusion

The successful utilization of AgNPs-GSE in bacterial photoinactivation has been attributed to their antibacterial properties and non-toxic nature. AgNPs-GSE at 2 mM significantly increased the percentage of *E. coli* bacterial death by 67% and *S. aureus* bacterial death by 69.01%. AgNPs-GSE demonstrated superior efficacy against gram-positive bacteria due to their susceptible cell walls, while blue laser irradiation at 405 nm led to bacterial death in both treatment groups. In the treatment group without AgNPs-GSE, *E. coli* exhibited a death rate of 27.45%, while *S. aureus* showed a rate of 29.19% after 180 seconds of irradiation. Conversely, in the treatment group with the addition of AgNPs-GSE at 2 mM, *E. coli* experienced a death rate of 83.80%, and AgNPs-GSE at 1 mM reduced the population of *S. aureus* by 87.01% with 180 seconds of irradiation. The photoinactivation potential achieved with 405 nm blue laser irradiation, both with and without AgNPs-GSE, was most effective at a dose of 3.44 J/cm^2 in reducing the populations of *E. coli* and *S. aureus* bacteria.

Acknowledgments

The authors would like to thank the Institute of Engineering and Engineering Life Sciences Airlangga University, Indonesia, for funding the research (no. 129/UN3.LIHTR/PT.01.05/2023).

Authors' Contribution

Conceptualization: Ahmad Khalil Yaqubi, Suryani Dyah Astuti, Andi Hamim Zaidan, Dezy Zahrotul Istiqomah Nurdin.
Data curation: Ahmad Khalil Yaqubi, Suryani Dyah Astuti.
Formal analysis: Ahmad Khalil Yaqubi, Suryani Dyah Astuti, Andi Hamim Zaidan
Funding acquisition: Suryani Dyah Astuti.
Investigation: Ahmad Khalil Yaqubi.
Methodology: Ahmad Khalil Yaqubi, Suryani Dyah Astuti, Andi Hamim Zaidan.
Project administration: Ahmad Khalil Yaqubi, Suryani Dyah Astuti, Dezy Zahrotul Istiqomah Nurdin.
Resources: Ahmad Khalil Yaqubi, Suryani Dyah Astuti, Andi Hamim Zaidan.
Software: Ahmad Khalil Yaqubi, Dezy Zahrotul Istiqomah Nurdin.
Supervision: Suryani Dyah Astuti, Andi Hamim Zaidan.
Validation: Ahmad Khalil Yaqubi, Suryani Dyah Astuti, Andi Hamim Zaidan, Dezy Zahrotul Istiqomah Nurdin.
Visualization: Ahmad Khalil Yaqubi, Suryani Dyah Astuti, Andi Hamim Zaidan, Dezy Zahrotul Istiqomah Nurdin.
Writing–original draft: Ahmad Khalil Yaqubi.
Writing–review & editing: Ahmad Khalil Yaqubi, Suryani Dyah Astuti.

Competing Interests

The authors declare no conflict of interest.

Ethical Approval

Not applicable.

Funding

None.

References

1. Kolahalam LA, Kasi Viswanath IV, Diwakar BS, Govindh B, Reddy V, Murthy YLN. Review on nanomaterials: synthesis and applications. Mater Today Proc. 2019;18(Pt 6):2182-90. doi: 10.1016/j.matpr.2019.07.371.
2. Singh C, Sharma V, Naik PK, Khandelwal V, Singh H. A green biogenic approach for synthesis of gold and silver nanoparticles using *Zingiber officinale*. Dig J Nanomater Biostruct. 2011;6(2):535-42.
3. Altammar KA. A review on nanoparticles: characteristics, synthesis, applications, and challenges. Front Microbiol. 2023;14:1155622. doi: 10.3389/fmicb.2023.1155622.
4. Maduraimuthu V, Ranishree JK, Gopalakrishnan RM, Ayyadurai B, Raja R, Heese K. Antioxidant activities of photoinduced phycogenic silver nanoparticles and their potential applications. Antioxidants. 2023;12(6):1298. doi: 10.3390/antiox12061298.
5. Hermosilla E, Díaz M, Vera J, Seabra AB, Tortella G, Parada J, et al. Molecular weight identification of compounds involved in the fungal synthesis of AgNPs: effect on antimicrobial and photocatalytic activity. Antibiotics (Basel). 2022;11(5):622. doi: 10.3390/antibiotics11050622.
6. Corrales M, Han JH, Tauscher B. Antimicrobial properties of grape seed extracts and their effectiveness after incorporation into pea starch films. Int J Food Sci Technol. 2009;44(2):425-33. doi: 10.1111/j.1365-2621.2008.01790.x.
7. Sochorova L, Prusova B, Cebova M, Jurikova T, Mlcek J, Adamkova A, et al. Health effects of grape seed and skin extracts and their influence on biochemical markers. Molecules. 2020;25(22):5311. doi: 10.3390/molecules25225311.
8. Xiao P, Li H, Wang T, Xu X, Li J, Zhu J. Efficient Fenton-like La–Cu–O/SBA-15 catalyst for the degradation of organic dyes under ambient conditions. RSC Adv. 2014;4(24):12601-4. doi: 10.1039/c4ra00917g.
9. Malik S, Muhammad K, Waheed Y. Nanotechnology: a revolution in modern industry. Molecules. 2023;28(2):661. doi: 10.3390/molecules28020661.
10. Okafor F, Janen A, Kukhtareva T, Edwards V, Curley M. Green synthesis of silver nanoparticles, their characterization, application and antibacterial activity. Int J Environ Res Public Health. 2013;10(10):5221-38. doi: 10.3390/ijerph10105221.
11. Sinha SN, Paul D. Phytosynthesis of silver nanoparticles using *Andrographis paniculata* leaf extract and evaluation of their antibacterial activities. Spectrosc Lett. 2015;48(8):600-4. doi: 10.1080/00387010.2014.938756.
12. He C, Liu L, Fang Z, Li J, Guo J, Wei J. Formation and characterization of silver nanoparticles in aqueous solution via ultrasonic irradiation. Ultrason Sonochem. 2014;21(2):542-8. doi: 10.1016/j.ultsonch.2013.09.003.
13. Pathrose B, Nampoori VPN, Radhakrishnan P, Sahira H, Mujeeb A. Effect of femtosecond laser ablated silver nanoparticles in the thermo-optic properties of basic fuchsin dye. Optik. 2016;127(7):3684-7. doi: 10.1016/j.ijleo.2016.01.016.
14. Fisenko SP, Khodyko JA. Low pressure evaporative cooling of micron-sized droplets of solutions and its novel applications. Int J Heat Mass Transf. 2009;52(15-6):3842-9. doi: 10.1016/j.ijheatmasstransfer.2009.02.017.
15. Zhang X, Xu S, Jiang S, Wang J, Wei J, Xu S, et al. Growth graphene on silver–copper nanoparticles by chemical vapor deposition for high-performance surface-enhanced Raman scattering. Appl Surf Sci. 2015;353:63-70. doi: 10.1016/j.apsusc.2015.06.084.
16. Astuti SD, Hafidiana, Rulaningtyas R, Abdurachman, Putra AP, Samian, et al. The efficacy of photodynamic inactivation with laser diode on *Staphylococcus aureus* biofilm with various ages of biofilm. Infect Dis Rep. 2020;12(Suppl 1):8736. doi: 10.4081/idr.2020.8736.
17. Raj KP, Sadayandi K. Effect of temperature on structural, optical and photoluminescence studies on ZnO nanoparticles synthesized by the standard co-precipitation method. Physica B Condens Matter. 2016;487:1-7. doi: 10.1016/j.

physb.2016.01.020.
18. Ivanova T, Harizanova A, Koutzarova T, Vertruyen B. Optical and structural characterization of TiO2 films doped with silver nanoparticles obtained by sol–gel method. Opt Mater (Amst). 2013;36(2):207-13. doi: 10.1016/j.optmat.2013.08.030.
19. Zahoranová T, Mori T, Yan P, Ševčíková K, Václavů M, Matolín V, et al. Study of the character of gold nanoparticles deposited onto sputtered cerium oxide layers by deposition-precipitation method: influence of the preparation parameters. Vacuum. 2015;114:86-92. doi: 10.1016/j.vacuum.2015.01.005.
20. Hu B, Wang SB, Wang K, Zhang M, Yu SH. Microwave-assisted rapid facile "green" synthesis of uniform silver nanoparticles: self-assembly into multilayered films and their optical properties. J Phys Chem C. 2008;112(30):11169-74. doi: 10.1021/jp801267j.
21. Ahmad A, Senapati S, Khan MI, Kumar R, Ramani R, Srinivas V, et al. Intracellular synthesis of gold nanoparticles by a novel alkalotolerant actinomycete, *Rhodococcus* species. Nanotechnology. 2003;14(7):824. doi: 10.1088/0957-4484/14/7/323.
22. Ping Y, Zhang J, Xing T, Chen G, Tao R, Choo KH. Green synthesis of silver nanoparticles using grape seed extract and their application for reductive catalysis of Direct Orange 26. J Ind Eng Chem. 2018;58:74-9. doi: 10.1016/j.jiec.2017.09.009.
23. Tran HV, Chu AD, Van Nguyen T, Nguyen ND, Le TD, Huynh CD. An investigation of silver nanoparticles formation under presence of graphene quantum dots as reducing reagent and stabilizer. Mater Trans. 2018;59(7):1106-11. doi: 10.2320/matertrans.MD201713.
24. Perumal D, Khairuddin NF, Wong JH, Abdullah CA. Plant extract-based silver nanoparticles and their bioactiviy investigations. In: Diversity and Applications of New Age Nanoparticles. IGI Global; 2023. p. 88-111. doi: 10.4018/978-1-6684-7358-0.ch004.
25. Park CM, Heo J, Yoon Y. Oxidative degradation of bisphenol A and 17α-ethinyl estradiol by Fenton-like activity of silver nanoparticles in aqueous solution. Chemosphere. 2017;168:617-22. doi: 10.1016/j.chemosphere.2016.11.016.
26. Al-Otibi F, Alkhudhair SK, Alharbi RI, Al-Askar AA, Aljowaie RM, Al-Shehri S. The antimicrobial activities of silver nanoparticles from aqueous extract of grape seeds against pathogenic bacteria and fungi. Molecules. 2021;26(19):6081. doi: 10.3390/molecules26196081.
27. Vijayakumar G, Kim HJ, Rangarajulu SK. In vitro antibacterial and wound healing activities evoked by silver nanoparticles synthesized through probiotic bacteria. Antibiotics (Basel). 2023;12(1):141. doi: 10.3390/antibiotics12010141.
28. Paschoal MA, Tonon CC, Spolidório DM, Bagnato VS, Giusti JS, Santos-Pinto L. Photodynamic potential of curcumin and blue LED against *Streptococcus mutans* in a planktonic culture. Photodiagnosis Photodyn Ther. 2013;10(3):313-9. doi: 10.1016/j.pdpdt.2013.02.002.
29. Chandra J, Mukherjee PK, Ghannoum MA. Fungal biofilms in the clinical lab setting. Curr Fungal Infect Rep. 2010;4(3):137-44. doi: 10.1007/s12281-010-0020-z.
30. Astuti SD, Mawaddah A, Nasution AM, Mahmud AF, Fitriyah N, Kusumawati I, et al. Effectiveness of photodynamic inactivation with exogenous photosensitizer *Curcuma longa* extract activated by laser diode 403 nm on *Staphylococcus aureus*. J Int Dent Med Res. 2020;13(1):155-61.
31. Felifel NT, Sliem MA, Kamel Z, Bojarska J, Seadawy MG, Amin RM, et al. Antimicrobial photodynamic therapy against *Escherichia coli* and *Staphylococcus aureus* using nanoemulsion-encapsulated zinc phthalocyanine. Microorganisms. 2023;11(5):1143. doi: 10.3390/microorganisms11051143.
32. Numai T. Fundamentals of semiconductor lasers. In: Fundamentals of Semiconductor Lasers. Tokyo: Springer; 2015. p. 89-186. doi: 10.1007/978-4-431-55148-5_5.
33. Astuti SD, Widya IW, Arifianto D, Apsari R. Effectiveness photodynamic inactivation with wide spectrum range of diode laser to *Staphylococcus aureus* bacteria with endogenous photosensitizer: an in vitro study. J Int Dent Med Res. 2019;12(2):481-6.
34. Mardianto AI, Setiawatie EM, Lestari WP, Rasheed A, Astuti SD. Photodynamic inactivation of *Streptococcus mutan* bacteri with photosensitizer *Moringa oleifera* activated by light emitting diode (LED). J Phys Conf Ser. 2020;1505(1):012061. doi: 10.1088/1742-6596/1505/1/012061.
35. Vishwanath R, Negi B. Conventional and green methods of synthesis of silver nanoparticles and their antimicrobial properties. Curr Res Green Sustain Chem. 2021;4:100205. doi: 10.1016/j.crgsc.2021.100205.
36. Rozykulyyeva L, Astuti SD, Zaidan AH, Pradhana AAS, Puspita PS. Antibacterial activities of green synthesized silver nanoparticles from *Punica granatum* peel extract. AIP Conf Proc. 2020;2314(1):060012. doi: 10.1063/5.0034126.
37. Lei J, Xin C, Xiao W, Chen W, Song Z. The promise of endogenous and exogenous riboflavin in anti-infection. Virulence. 2021;12(1):2314-26. doi: 10.1080/21505594.2021.1963909.
38. Ormond AB, Freeman HS. Dye sensitizers for photodynamic therapy. Materials (Basel). 2013;6(3):817-40. doi: 10.3390/ma6030817.
39. Kempa M, Kozub P, Kimball J, Rojkiewicz M, Kuś P, Gryczyński Z, et al. Physicochemical properties of potential porphyrin photosensitizers for photodynamic therapy. Spectrochim Acta A Mol Biomol Spectrosc. 2015;146:249-54. doi: 10.1016/j.saa.2015.03.076.
40. Maraccini PA, Wenk J, Boehm AB. Photoinactivation of Eight Health-Relevant Bacterial Species: Determining the Importance of the Exogenous Indirect Mechanism. Environ Sci Technol. 2016;50(10):5050-5059. doi:10.1021/acs.est.6b00074.
41. Astuti SD, Wibowo RA, Abdurachman NI, Triyana K. Antimicrobial photodynamic effects of polychromatic light activated by magnetic fields to bacterial viability. J Int Dent Med Res. 2017;10(1):111-7.
42. Astuti SD, Mahmud AF, Pudjiyanto, Mukhammad Y, Fitriyah N. Antimicrobial photodynamic of blue LED for activation of curcumin extract (*Curcuma longa*) on *Staphylococcus aureus* bacteria, an in vitro study. J Phys Conf Ser. 2018;1120(1):012073. doi: 10.1088/1742-6596/1120/1/012073.
43. Yaqubi AK, Astuti SD, Permatasari PA, Komariyah N, Endarko E, Zaidan AH. Effectiveness of purple led for inactivation of *Bacillus subtilis* and *Escherichia coli* bacteria in in vitro sterilizers. Biomedical Photonics. 2022;11(4):4-10. doi: 10.24931/2413–9432–2022–11-4-4-10.
44. Szymczak K, Szewczyk G, Rychłowski M, Sarna T, Zhang L, Grinholc M, et al. Photoactivated gallium porphyrin reduces *Staphylococcus aureus* colonization on the skin and suppresses its ability to produce enterotoxin C and TSST-1. Mol Pharm. 2023;20(10):5108-24. doi: 10.1021/acs.molpharmaceut.3c00399.
45. Halliwell B. Reactive species and antioxidants. Redox biology is a fundamental theme of aerobic life. Plant Physiol. 2006;141(2):312-22. doi: 10.1104/pp.106.077073.
46. Astuti SD, Kharisma DH, Kholimatussadiah S, Zaidan AH. An in vitro antifungal efficacy of silver nanoparticles activated by diode laser to *Candida albicans*. AIP Conf Proc. 2017;1888(1):020016. doi: 10.1063/1.5004293.